Published in final edited form as:
J Neuropathol Exp Neurol. 2008 August ; 67(8): 784–792. doi:10.1097/NEN.0b013e318180f0d5.

Productive SV40 Infection of Neurons in Immunosuppressed Rhesus Monkeys

Xin Dang, PhD[1], **Christian Wüthrich, PhD**[1], **Michael K. Axthelm, DVM, PhD**[3,4], and **Igor J. Koralnik, MD**[1,2,*]

[1] Division of Viral Pathogenesis, Beth Israel Deaconess Medical Center, Harvard Medical School, Boston, Massachusetts

[2] Department of Neurology, Beth Israel Deaconess Medical Center, Harvard Medical School, Boston, Massachusetts

[3] Vaccine and Gene Therapy Institute, Oregon National Primate Research Center, Oregon Health and Science University, Beaverton, Oregon

[4] Division of Pathobiology and Immunology, Oregon National Primate Research Center, Oregon Health and Science University, Beaverton, Oregon

Abstract

There currently is no animal model of JC virus (JCV)-associated progressive multifocal leukoencephalopathy (PML). Reactivation of simian virus-40 (SV40) in immunosuppressed rhesus monkeys, however, rarely causes a PML-like illness. We sought to isolate a neurotropic clone of SV40 and determine its pathogenic potential in monkeys. The clone $SV40_{CNS1}$ was amplified by PCR from the brain DNA of a simian/human immunodeficiency virus (SHIV)-infected monkey that had developed PML and meningoencephalitis. $SV40_{CNS1}$ had a small number of single amino acid mutations compared to the SV40 prototype 776 and caused a productive infection in monkey fibroblasts. It was inoculated into two SV40-negative, SHIV-immunosuppressed monkeys. Both animals developed meningoencephalitis with productive SV40 infection of cerebral cortical neurons and glia in the superficial layers of the cortex and at the gray-white junction. Focal SV40-infected cells were also found in the cerebellar molecular and granule cell layers and white matter. Both animals also developed disseminated SV40 infection with nephritis and pneumonitis. Thus, $SV40_{CNS1}$ is infectious and pathogenic in immunosuppressed monkeys, but it induces encephalitis with fulminant productive infection in cortical neurons and systemic disease rather than PML. These findings shed new light on SV40 neurotropism and expand the host cell range of this virus.

Keywords

Neuron infection; Progressive multifocal leukoencephalopathy (PML); Rhesus monkey; SV40

Correspondence and reprint requests to: Igor J. Koralnik, Division of Viral Pathogenesis, Beth Israel Deaconess Medical Center, RE-213C, 330 Brookline Avenue, Boston, MA, 02215. Telephone: (617) 667-1568; Fax: (617) 667-8210. E-mail: ikoralni@bidmc.harvard.edu.

This research was performed at Beth Israel Deaconess Medical Center (Boston) and Oregon National Primate Research Center (Beaverton).

INTRODUCTION

There is no specific treatment for progressive multifocal leukoencephalopathy (PML) which is caused by the polyomavirus JC (JCV) (1). Since JCV induces tumors in animals (2,3) and only causes PML in humans, our understanding of its pathogenesis has been hindered by the absence of an appropriate animal model. The simian virus 40 (SV40) has 69% sequence homology with JCV. Asymptomatic infection with JCV occurs in humans and, likewise, asymptomatic infection with SV40 is common in rhesus monkeys in the wild. Furthermore, reactivation of latent SV40 has been observed in 2.6% of simian immunodeficiency virus-infected monkeys and this is associated with a disease that resembles PML (4). This low rate of disease induction, however, precludes the use of SV40 in a monkey PML model. We previously studied primary SV40 infection by inoculating two SV40-negative immunosuppressed rhesus monkeys with a brain isolate of this virus and showed that both animals developed meningoencephalitis and a PML-like disease within 16 weeks (5). Detailed sequence analysis of SV40 from various compartments demonstrated that unlike JCV in humans, rearrangement of SV40 regulatory region was not necessary for the induction of PML (6). To investigate SV40 primary infection in immunosuppressed hosts further, we obtained a full-length clone from the brain of one of these animals and used it to inoculate two SV40-negative, simian/human immunodeficiency virus (SHIV)-immunosuppressed rhesus monkeys. Surprisingly, this clone caused widespread SV40 infection in the brains with a productive infection of cerebral cortical neurons and other cells and dissemination to non-CNS tissues,

MATERIALS AND METHODS

Isolation of the full-length $SV40_{CNS1}$ clone from the brain of a monkey with PML and meningoencephalitis

DNA was extracted from the brain of the SHIV-infected monkey 21289 diagnosed with a PML-like disease and meningoencephalitis after primary infection with SV40 isolate 18429. This isolate had been obtained from the brain of a monkey that developed PML as a reactivation of a natural SV40 infection (5). DNA samples were used for long polymerase chain reaction (PCR) amplification of SV40 as previously described (7). The PCR products were cloned into the cloning vector pUC18 (Invitrogen, Carlsbad, CA) and the entire nucleotide composition of the SV40 genome was verified by sequencing.

Transfection of $SV40_{CNS1}$ clone in monkey fibroblasts

One μg of linearized genomes of SV40 prototype 776 and $SV40_{CNS1}$, respectively, was used to transfect 0.6×10^6 telomerized monkey fibroblast cells (8) cultured in 6-well plates using Effectene Transfection Reagent (Qiagen, Germantown, MD). SV40-transfected cells were transferred to P175 flasks on day 15. Supernatants were harvested and medium was changed every three days starting on day 4 until the termination of the experiment and harvesting of the cells on day 30.

Western blot detection of SV40 major capsid protein VP1

Supernatant and cell lysates of transfected monkey fibroblasts were subjected to polyacrylamide gel electrophoresis. The Western blot was performed using anti-rJCVp1 (which cross reacts with SV40) polyclonal rabbit sera ([“14a bleed #4)”], a generous gift from Dr. Eugene Major) and a secondary goat anti-rabbit Ig conjugated with horseradish peroxidase (HRP; Dako, Carpinteria, CA). The film was developed with ECL Western blotting detection reagents (Amersham Pharmacia Biotech, Buckinghamshire, UK).

In vitro infection and verification of genomic stability of $SV40_{CNS1}$

One and a half ml of supernatants from the transfected monkey fibroblasts cultures were used to infect a 90% confluent P175 flask of monkey fibroblasts. Supernatant was harvested three days after infection; the virus was passaged five times after which both supernatant and cells were harvested. The SV40 regulatory region was PCR-amplified as previously described (6), and randomly selected clones were sequenced to verify the genomic stability of $SV40_{CNS1}$ in vitro.

Large-scale production of $SV40_{CNS1}$

Twenty P175 flasks of telomerized monkey fibroblasts (60%–80% confluent) were infected with 5 mL supernatant harvested during the transfection experiment and cells were harvested 21 days later. Cell lysates were subjected to three cycles of freezing and thawing, followed by sonication. SV40 virions were pelleted by centrifugation at 100,000 × g for 2 hours in Hanks buffer and stored at −80°C until use (5).

Experimental infection of SV40-negative rhesus monkeys with SHIV and $SV40_{CNS1}$

Rhesus macaques 22710 and 22756 were seronegative for simian immunodeficiency virus, simian T lymphotropic virus 1, D type simian retrovirus, simian spumaretrovirus, Cercopithecine herpesvirus 1, rhesus cytomegalovirus, rhesus rhadinovirus, rhesus lymphocryptovirus and SV40 and were housed at the Oregon National Primate Research Center and maintained in accordance with the guidelines of the Institutional Animal Care and Use Committee and the Guide for the Care and Use of Laboratory Animals (9). They were inoculated intravenously with 100 MID50 (approximately 150,000 RNA copies) of the highly pathogenic simian/human immunodeficiency hybrid virus SHIV 89.6-P (10) at 1 year and 321 days and 1 year and 206 days of age, respectively, as previously described (5). After 49 days the animals were infected intravenously with 10^7 plaque-forming units of $SV40_{CNS1}$. Monkeys with vomiting, dehydration and listlessness were killed at 115 and 108 days after SHIV infection and 66 and 59 days after $SV40_{CNS1}$ infection, respectively. Complete necropsy examinations were conducted.

Histological analyses and immunohistochemical staining for SV40 VP1 protein in monkey samples

Coronal sections of the brain and serial sections of the spinal cord were examined at 5 mm intervals. Other organs studied included the kidney, lung, lymph nodes, jejunum, liver, pancreas and parotid gland. Formalin-fixed, paraffin-embedded tissue sections were stained with hematoxylin and eosin for routine histological examination. Sections of kidney were also stained with periodic acid-Schiff (PAS) stain and Masson's trichrome. A Luxol fast blue (LFB)-PAS-eosin stain was performed for visualization of myelin in brain sections and for identification of macrophages.

Single and multiple immunohistochemistry

The following antibodies (Abs) were used for immunohistochemistry (IHC) and immunofluorescence: SV40 infected cells: mouse monoclonal anti-SV40 VP1, PAB597 and rabbit antisera against SV40 VP1 (Lee Biomolecular Research, San Diego, CA); Neurons: MAP-2 (M-4403; Sigma, St. Louis, MO) and NeuN (MAB377; Chemicon, Temecula, CA); Astrocytes: GFAP (M0761 and Z0334; Dako); Oligodendrocytes: CNPase (C5922; Sigma), MOSP (MAB328; Chemicon). Formalin-fixed, paraffin-embedded sections were baked for 2 hours and treated in an electric pressure-cooker for 15 minutes in Trilogy solution (Cell Marque, Hot Springs, AR) for deparaffinization, rehydration and antigen retrieval as previously described (11). For all wash steps, phosphate-buffered saline with 0.05% Tween 20 was used. A protein block (Dako) was used for 30 minutes before incubation with the primary Ab. After

primary Ab incubations, the Envision System/AP, Envision G/2 System/AP, Envision double stain, Envision G/2 double stain and Advance-HRP kits (Dako) were used according to the manufacturer's instructions. Sections were counterstained with hematoxylin and, when appropriate, with LFB stain for myelin before mounting. For HRP chromogen, endogenous peroxidase blocking solution was applied during 3 minutes before the protein block. Controls consisted of omission of the primary Abs and/or the use of healthy monkey tissues.

Single and multiple immunofluorescence

Immunofluorescence staining was done on formalin-fixed, paraffin-embedded samples as described in (12). Directly conjugated goat anti-mouse (IgG and/or IgM) and/or goat anti-rabbit (IgG) Alexa Fluor 350, 488 and 568 (Molecular Probes, Eugene, OR) secondary Abs were used according to the manufacturer's instructions.

RESULTS

Isolation of a full-length clone of SV40 from the brain of monkey 21289

The genomic map of $SV40_{CNS1}$ is shown in Figure 1. Compared to the SV40 prototype 776, the $SV40_{CNS1}$ regulatory region has only one 72 bp element instead of two, similar to the archetype SV40 regulatory region. In addition, the coding region of $SV40_{CNS1}$ has a total of 10 silent single-nucleotide mutations scattered in VP1, VP2, VP3, and T genes. Seven amino acid mutations in VP1 (n = 1), t (n = 2) and T genes (n = 4) and were previously reported (13–16), except that the adenine to cytosine change located at nt position 1756 (according to SV40 776 numbering) resulting in amino acid change of E to D in the VP1 protein (Table). A 3-bp deletion in the inter-coding region between T and VP1 genes from nt 2677 to 2679 (following the SV40 776 numbering) was also found; the latter had no influence on protein expression.

$SV40_{CNS1}$ clone is infectious and replicates in monkey fibroblasts

When probed with an Ab against the major capsid protein VP1, a band of approximately 40 kDa was detected by Western blot in both supernatant and cell lysate samples obtained from either the SV40 prototype strain 776 or $SV40_{CNS1}$-transfected monkey fibroblasts (Fig. 2). The presence of this protein and the fact that supernatant of $SV40_{CNS1}$-transfected monkey fibroblasts could be used to infect naive fibroblasts indicated that $SV40_{CNS1}$ was able to undergo a full replicative cycle in these cells, consistent with the production of mature viral particles.

$SV40_{CNS1}$ is infectious in vitro and has a stable regulatory region

To determine the stability of the $SV40_{CNS1}$ strain, the regulatory region was amplified by PCR, cloned and sequenced from five successive passages of the virus in monkey fibroblasts. High titers of $SV40_{CNS1}$ virus were obtained (>15,000 TCID50/ml). No change was found in the $SV40_{CNS1}$ regulatory region over time, indicating that $SV40_{CNS1}$ was both infectious and stable in vitro.

$SV40_{CNS1}$ is infectious and pathogenic in vivo

SV40-seronegative monkeys 22710 and 22756 were inoculated IV with $SV40_{CNS1}$ 49 days post-SHIV infection, a time point when they were severely immunosuppressed as demonstrated by $CD4^+$ T cell counts below $10/mm^3$ (Fig. 3A). Both animals showed a steady increase in SV40 DNA viral load in peripheral blood mononuclear cells (PBMCs) until it reached a plateau around 10^4 copies of SV40/mg of PBMC DNA three weeks later; this remained stable until the time of death (Fig. 3B).

Between 34 and 38 days post-SV40 inoculation, both animals showed reduced appetite; they developed emesis between days 55 and 61, which led to progressive dehydration and electrolyte alterations. Additionally, monkey 22756 had an elevated blood urea nitrogen (81 mg/dL, normal 9–24), hyperphosphatemia (11.9 mg/dL, normal 3.0–3.5), elevated serum alanine transferase (102 IU/L, normal 0–37), and elevated serum aspartate transferase (124 IU/L, normal 5–40) on post-SV40 inoculation day 55. The animals were killed at days 59 and 66 after SV40 infection (Fig. 3). Gross examination of their brains revealed distension of the subarachnoid spaces with excessive fluid. The cerebral convexities were pale and had flattened gyri. Spinal cords were unremarkable. Postmortem examination revealed weight loss (10%–25%), generalized lymphoid and thymic atrophy, multifocal lung consolidation, segmentally edematous small and large bowel and serous peritoneal effusions. The kidneys were swollen and had pale streaks extending from the capsular surface through the cortices on sectioning. Additionally, the gall bladder, extrahepatic bile duct, and pancreatic duct were distended and thickened in monkey 22756.

Histology

Both monkeys had diffuse, severe, subacute encephalomyelitis characterized by profound, generalized subpial edema in cerebral molecular and external granular cell layers. This was accompanied by prominent gemistocytic astrocytes, many with enlarged, bizarre, multicoated nuclei, microglial activation and sparse lymphocytes. Mild meningitis consisted of sparse lymphocytic infiltration and fibroblast proliferation in the subarachnoid space. Smudgy amphophilic intranuclear inclusions were evident in subarachnoid cells and in gemistocytic astrocytes and neurons in the superficial and deep cortical layers. Intermediate cortical zones were largely spared (Fig. 4A).

Astrocyte and neuron infection in the deep cortical and U fiber regions was accompanied by scattered oligodendrocyte infection in adjacent white matter with occasional foci of early demyelination. Less frequently there was multifocal subependymal edema adjacent to the lateral and third ventricles. There were scattered glial cells with amphophilic intranuclear inclusions in the subependymal plate and periventricular gray matter and in the infundibulum (Fig. 4B). Intranuclear inclusions were observed in occasional tela choroidea stromal cells but not in epithelial or ependymal cells. Oligodendrocytes and astrocytes in the optic chiasm and olfactory tracts also had intranuclear inclusions (not shown).

Double IHC staining for neurons and SV40 VP1 confirmed the presence of SV40-infected cells in meninges and superficial and deep cortical layers. These included meningeal cells, glia and neurons in either the cortex or subcortical white matter (Fig. 5A–D).

Immunofluorescence staining for GFAP and SV40 VP1 showed that astrocytes constituted the majority of SV40-infected cells in the superficial and deep layers of the cortex, which could occasionally be found along vessels in mid cortex (Fig. 6).

To differentiate SV40-infected cells in the cerebral cortex further, we performed triple IHC staining for neurons, astrocytes and SV40 VP1. As shown in Figure 7, SV40-infected neurons and astrocytes could sometimes be found in close proximity. In addition, a double IHC experiment using a second neuronal Ab and an anti-SV40 VP1 Ab confirmed the presence of SV40-infected neurons in the cerebral cortex (Fig. 7).

Microscopic evidence of SV40 infection in the cerebellum was confined to clusters of cells with enlarged nuclei containing smudgy amphophilic inclusions in the absence of inflammation in the molecular and granular cell layers. This was confirmed by IHC staining for SV40 VP1 (Fig. 8A). In addition, few PML-like lesions with SV40-infected cells were present in the cerebellar white matter (Fig. 8B)

The systemic histological findings were the same in both animals. They included severe subacute tubulointerstitial nephritis at the level of Henle's loop and collecting ducts. The tubular epithelial cells had enlarged nuclei that stained positively for SV40 by IHC (Fig. 9A, B). Moderate numbers of lymphocytes and plasma cells and occasional neutrophils infiltrated the interstitium.

Generalized depletion of lymphocytes in lymph nodes, spleen and the thymus was accompanied by sinus histiocytosis in most lymph nodes. Varying numbers of reticuloendothelial cells and macrophages with intranuclear inclusions were present in depleted cortex, medullary cords and lymph node sinuses in both animals and in the depleted, condensed thymic cortical stroma of monkey 22756. The inclusions stained positively for SV40 (Fig. 9C, D). Smudgy, basophilic to amphophilic intranuclear inclusions were also present in plump fusiform cells in the splenic sinusoids and splenic trabecular smooth muscle cells.

Severe, subacute, multifocal interstitial pneumonia was characterized by patchy alveolar and small airway epithelial damage and prominent type II pneumocyte hyperplasia. Focally, pneumocytes had enlarged nuclear and smudgy basophilic intranuclear inclusions that were immunopositive for SV40 (Fig. 9E, F).

Gastrointestinal tract involvement included basophilic intranuclear inclusions in ganglion cells in Auerbach and Meissner plexuses and in smooth muscle and fusiform mesenchymal cells in the subserosa and submucosa (not shown). Both monkeys had enteric cryptosporidiosis and monkey 22756 also had cryptosporidial infection of the bile and pancreatic ducts. Other organs and tissues sites with infected parenchymal cells included Kupffer's cells in the liver and duct epithelial cells in the parotid gland and pancreas (not shown).

DISCUSSION

The cornerstone of an animal model of a viral infection resides in the isolation of an infectious and pathogenic clone of the virus. The $SV40_{CNS1}$ clone was isolated from the brain of an immunosuppressed rhesus monkey that developed meningoencephalitis and a PML-like disease nine weeks after primary infection with SV40 (5). The $SV40_{CNS1}$ regulatory region is archetypal as it is consistent with the predominant regulatory region found in brain, kidney and blood of this animal at the time of death (6). In addition, sequence analysis of the coding region of the $SV40_{CNS1}$ clone showed only single amino acid mutations compared to SV40 prototype 776, all of which have been reported separately in SV40 isolates (4,13,15,16), although never in combination. Furthermore, the $SV40_{CNS1}$ regulatory region remained stable after five passages of replication in monkey cells.

Although $SV40_{CNS1}$ has the same molecular characteristics as the PML isolate of SV40 used in our previous studies (5,6), primary infection in SHIV-immunosuppressed animals resulted in a more widespread infection that included meningoencephalitis, nephritis and pneumonitis rather than PML. This is consistent previous observations in SV40 primary infection occurring naturally in immunosuppressed monkeys (4). We describe here for the first time, however, detection of the major capsid protein VP1 in these cells, indicating that a full viral replicative cycle has occurred in neurons; this is consistent with productive infection. Although the host cell range of SV40 is much broader than that of JCV, SV40 infection of neurons has no previously been reported. It is therefore possible that the purified $SV40_{CNS1}$ clone is more neuronotropic than the brain isolate that had been used until this time (5). Interestingly, in vitro studies have shown that MHC class I proteins (17) and ganglioside GM1 (18) are cell surface receptors for SV40. Since neurons do not express MHC class I proteins (19,20) (although they may be upregulated in viral encephalitis), our findings suggest that the latter were likely the port of entry of SV40 in neurons.

SV40 infection of neurons was unexpected but it provides us with a unique window on the route of CNS invasion by SV40. Indeed, the viral infection of the CNS may initially affect the meninges, spread to astrocytes and neurons in the superficial layers of the cerebral cortex, and then extend to glial cells and neurons at the gray-white junction. Furthermore, foci of SV40 infection were seen in the molecular layer of the cerebellum, extending to the granule cell layer, and in some cases, forming demyelinating lesions in the cerebellar white matter. In this regard, we previously described a productive infection of granule cell neurons of the cerebellum by JCV (21,22). These data suggest that both SV40 and JCV may, in certain circumstances, infect neuronal cells, in addition to astrocytes and oligodendrocytes. How polyomaviruses might utilize the cell machinery for viral DNA replication in post-mitotic neurons deserves further study.

Approximately 100 million people worldwide were unwittingly infected by SV40-contaminated polio vaccines between 1955 and 1963. SV40 is oncogenic in animals and its persistence in human populations as well as its role as an emerging pathogen is a matter of debate (23,24). It has been associated with primary human neoplasms of the brain, bone, and pleura and with non-Hodgkin's lymphoma. Thus, our findings that both cortical hemispheric and cerebellar neurons can sustain SV40 infection in a species closely related to humans may have implications for the pathogenesis of this virus in human populations.

Finally, this model differs from most cases of PML in humans in that this disease is thought to occur principally as a reactivation of JCV in the setting of immunosuppression. The model may, however, be more relevant to cases of primary infection by JCV in immunosuppressed individuals, some of which may develop into PML (25). In addition, JCV meningitis or meningoencephalitis have been reported in a patient with systemic lupus erythematosus (26) and an immunocompetent child (27), possibly as a manifestation of JCV primary infection. Interestingly, the pathological findings in this report (i.e. meningoencephalitis, nephritis, and pneumonitis) share features with those in immunosuppressed individuals diagnosed with the polyomavirus BK (BKV) infection (28–32). BKV shares 75% sequence homology with SV40, and, as is the case for JCV, serology testing is not available outside of research laboratories. Furthermore, JCV and BKV PCR or IHC are not routinely performed on cerebrospinal fluid and brain samples, respectively, in cases of meningoencephalitis that lack demyelination. It is possible, therefore, primary infection with JCV or BKV as a cause of meningitis or encephalitis may be underdiagnosed.

PML used to be restricted to severely immunosuppressed individuals with AIDS, hematological malignancies or organ transplant recipients. More recently, it was reported in patients with multiple sclerosis and Crohn's disease who had been treated with the novel immunomodulatory medication natalizumab (33). Since the numbers of patients at risk for PML continues to increase, the development of an animal model remains a priority. Experiments are now in progress to determine whether infection of rhesus monkeys with the $SV40_{CNS1}$ clone followed by immunosuppression leads to a disease that shares more features with human PML.

Acknowledgments

This study was supported by NIH grant R21 046243 to IJK, NIH grant U24 018107 to MKA and NIH grant P51 RR00163 supporting the Oregon National Primate Research Center.

References

1. Koralnik IJ. Progressive multifocal leukoencephalopathy revisited: Has the disease outgrown its name? Ann Neurol 2006;60:162–73. [PubMed: 16862584]

2. Miller NR, McKeever PE, London W, et al. Brain tumors of owl monkeys inoculated with JC virus contain the JC virus genome. J Virol 1984;49:848–56. [PubMed: 6321769]
3. London WT, Houff SA, McKeever PE, et al. Viral-induced astrocytomas in squirrel monkeys. Prog Clin Biol Res 1983;105:227–37. [PubMed: 6304760]
4. Simon MA, Ilyinskii PO, Baskin GB, et al. Association of simian virus 40 with a central nervous system lesion distinct from progressive multifocal leukoencephalopathy in macaques with AIDS. Am J Pathol 1999;154:437–46. [PubMed: 10027402]
5. Axthelm MK, Koralnik IJ, Dang X, et al. Meningoencephalitis and demyelination are pathologic manifestations of primary polyomavirus infection in immunosuppressed rhesus monkeys. J Neuropathol Exp Neurol 2004;63:750–58. [PubMed: 15290900]
6. Dang X, Axthelm MK, Letvin NL, Koralnik IJ. Rearrangement of simian virus 40 regulatory region is not required for induction of progressive multifocal leukoencephalopathy in immunosuppressed rhesus monkeys. J Virol 2005;79:1361–66. [PubMed: 15650162]
7. Lednicky JA, Butel JS. Tissue culture adaptation of natural isolates of simian virus 40: changes occur in viral regulatory region but not in carboxy-terminal domain of large T-antigen. J Gen Virol 1997;78:1697–705. [PubMed: 9225047]
8. Kirchoff V, Wong S, St JS, Pari GS. Generation of a life-expanded rhesus monkey fibroblast cell line for the growth of rhesus rhadinovirus (RRV). Arch Virol 2002;147:321–33. [PubMed: 11890526]
9. Guide for the care and use of laboratory animals. (NIH) 85–23. Bethesda, MD: National Institutes of Health; 1985.
10. Reimann KA, Li JT, Veazey R, et al. A chimeric simian/human immunodeficiency virus expressing a primary patient human immunodeficiency virus type 1 isolate env causes an AIDS-like disease after in vivo passage in rhesus monkeys. J Virol 1996;70:6922–28. [PubMed: 8794335]
11. Kim WK, Corey S, Chesney G, et al. Identification of T lymphocytes in simian immunodeficiency virus encephalitis: Distribution of CD8+ T cells in association with central nervous system vessels and virus. J Neurovirol 2004;10:315–25. [PubMed: 15385254]
12. Williams KC, Corey S, Westmoreland SV, et al. Perivascular macrophages are the primary cell type productively infected by simian immunodeficiency virus in the brains of macaques: Implications for the neuropathogenesis of AIDS. J Exp Med 2001;193:905–15. [PubMed: 11304551]
13. Ilyinskii PO, Daniel MD, Horvath CJ, Desrosiers RC. Genetic analysis of simian virus 40 from brains and kidneys of macaque monkeys. J Virol 1992;66:6353–60. [PubMed: 1328671]
14. Stewart AR, Lednicky JA, Benzick US, et al. Identification of a variable region at the carboxy terminus of SV40 large T-antigen. Virology 1996;221:355–61. [PubMed: 8661447]
15. Lednicky JA, Arrington AS, Stewart AR, et al. Natural isolates of simian virus 40 from immunocompromised monkeys display extensive genetic heterogeneity: New implications for polyomavirus disease. J Virol 1998;72:3980–90. [PubMed: 9557685]
16. Newman JS, Baskin GB, Frisque RJ. Identification of SV40 in brain, kidney and urine of healthy and SIV-infected rhesus monkeys [see comments]. J Neurovirol 1998;4:394–406. [PubMed: 9718131]
17. Atwood WJ, Norkin LC. Class I major histocompatibility proteins as cell surface receptors for simian virus 40. J Virol 1989;63:4474–77. [PubMed: 2476575]
18. Tsai B, Gilbert JM, Stehle T, et al. Gangliosides are receptors for murine polyoma virus and SV40. Embo J 2003;22:4346–55. [PubMed: 12941687]
19. Lampson LA, Hickey WF. Monoclonal antibody analysis of MHC expression in human brain biopsies: Tissue ranging from “histologically normal” to that showing different levels of glial tumor involvement. J Immunol 1986;136:4054–62. [PubMed: 2422272]
20. Joly E, Mucke L, Oldstone MB. Viral persistence in neurons xplained by lack of major histocompatibility class I expression. Science 1991;253:1283–85. [PubMed: 1891717]
21. Du Pasquier RA, Corey S, Margolin DH, et al. Productive infection of cerebellar granule cell neurons by JC virus in an HIV+ individual. Neurology 2003;61:775–82. [PubMed: 14504320]
22. Koralnik IJ, Wuthrich C, Dang X, et al. JC virus granule cell neuronopathy: A novel clinical syndrome distinct from progressive multifocal leukoencephalopathy. Ann Neurol 2005;57:576–80. [PubMed: 15786466]
23. Vilchez RA, Butel JS. Emergent human pathogen simian virus 40 and its role in cancer. Clin Microbiol Rev 2004;17:495–508. [PubMed: 15258090]

24. Shah KV. SV40 and human cancer: a review of recent data. Int J Cancer 2007;120:215–23. [PubMed: 17131333]
25. Newman JT, Frisque RJ. Detection of archetype and rearranged variants of JC virus in multiple tissues from a pediatric PML patient. J Med Virol 1997;52:243–52. [PubMed: 9210031]
26. Viallard JF, Ellie E, Lazaro E, et al. JC virus meningitis in a patient with systemic lupus erythematosus. Lupus 2005;14:964–66. [PubMed: 16425577]
27. Blake K, Pillay D, Knowles W, et al. JC virus associated meningoencephalitis in an immunocompetent girl. Arch Dis Child 1992;67:956–57. [PubMed: 1325756]
28. Vallbracht A, Lohler J, Gossmann J, et al. Disseminated BK type polyomavirus infection in an AIDS patient associated with central nervous system disease. Am J Pathol 1993;143:29–39. [PubMed: 8391217]
29. Bratt G, Hammarin AL, Grandien M, et al. BK virus as the cause of meningoencephalitis, retinitis and nephritis in a patient with AIDS. AIDS 1999;13:1071–75. [PubMed: 10397537]
30. Cubukcu-Dimopulo O, Greco A, Kumar A, et al. BK virus infection in AIDS. Am J Surg Pathol 2000;24:145–49. [PubMed: 10632500]
31. Lesprit P, Chaline-Lehmann D, Authier FJ, et al. BK virus encephalitis in a patient with AIDS and lymphoma. Aids 2001;15:1196–99. [PubMed: 11416733]
32. Galan A, Rauch CA, Otis CN. Fatal BK polyoma viral pneumonia associated with immunosuppression. Hum Pathol 2005;36:1031–34. [PubMed: 16153469]
33. Berger JR, Koralnik IJ. Progressive multifocal leukoencephalopathy and natalizumAb--unforeseen consequences. N Engl J Med 2005;353:414–16. [PubMed: 15947082]

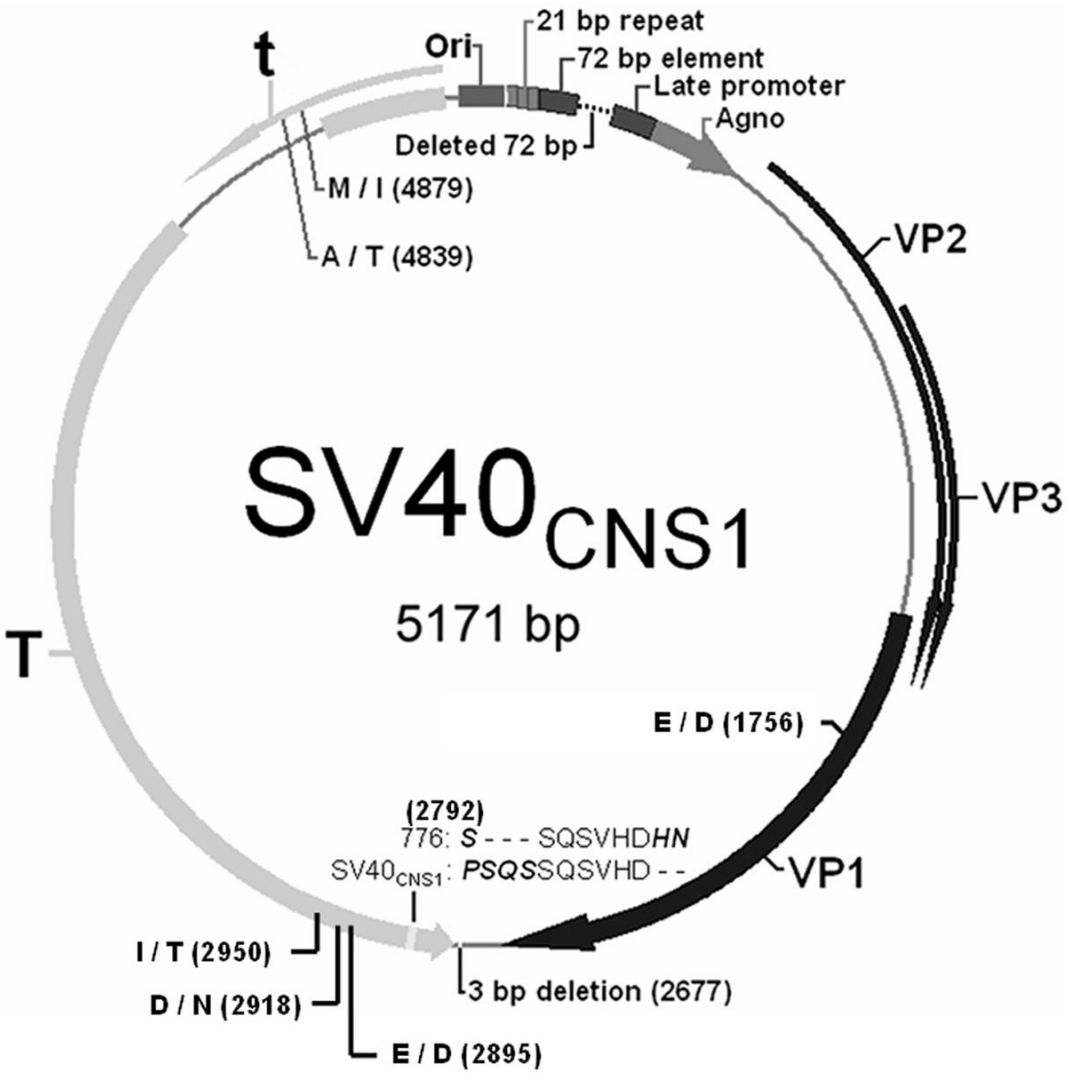

Figure 1.

Genomic map of $SV40_{CNS1}$. This 5171 bp circular, double-stranded DNA clone has a regulatory region (RR, top of circle) that contains a three 21 bp repeat structure and only one 72 bp element following the origin of replication (Ori). Early regulatory genes coding for t and T protein are on the left of the RR (light gray). Amino acid differences compared to SV40 776 (Table) are indicated. Genes coding for the agnoprotein (Agno, medium gray) and the capsid proteins VP1, VP2 and VP3 (black) are on the right of the RR.

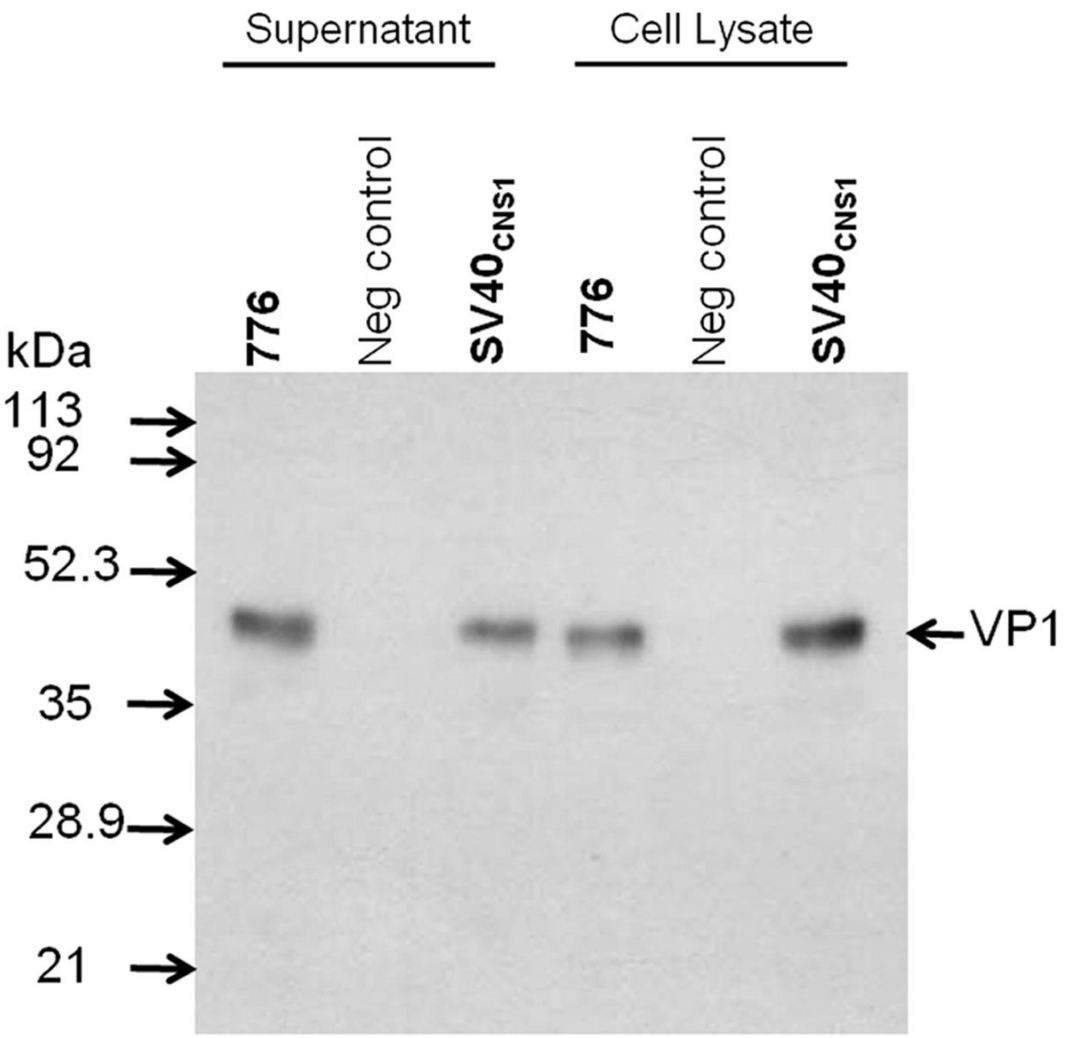

Figure 2.

Detection of $SV40_{CNS1}$ VP1 protein by Western blot. Supernatants and cell lysates of monkey fibroblast cell cultures transfected with SV40 776 or $SV40_{CNS1}$ DNA and uninfected cells (negative control) were tested by Western blot with an anti-JCV VP1 Ab that cross-reacts with SV40 VP1. Expected bands of approximately 40 kDa were detected in supernatant and lysates of both 776 and $SV40_{CNS1}$-transfected cell cultures, corresponding to the size of the VP1 protein.

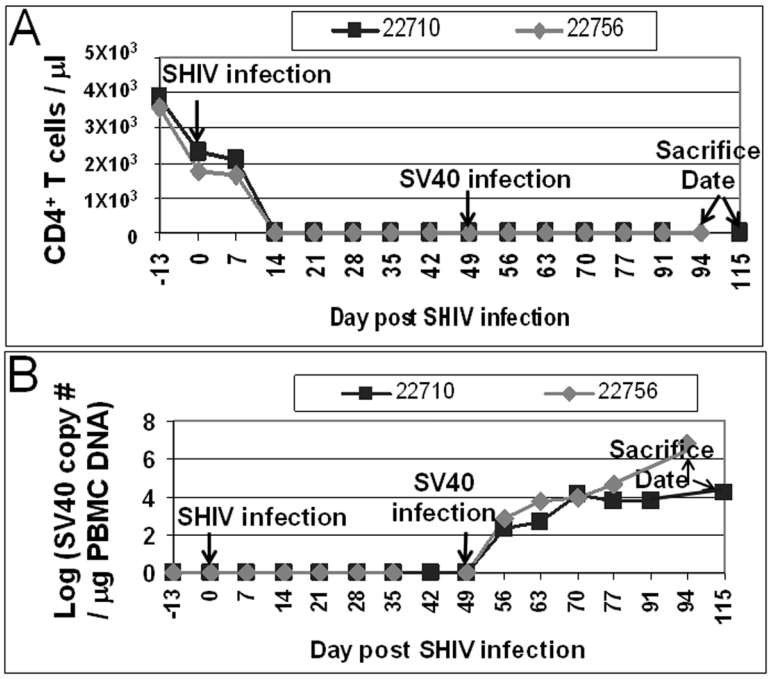

Figure 3.
Time plots of $CD4^+$ T lymphocyte counts (**A**) and SV40 DNA viral load (**B**) in PBMC samples of monkeys 22710 and 22756.

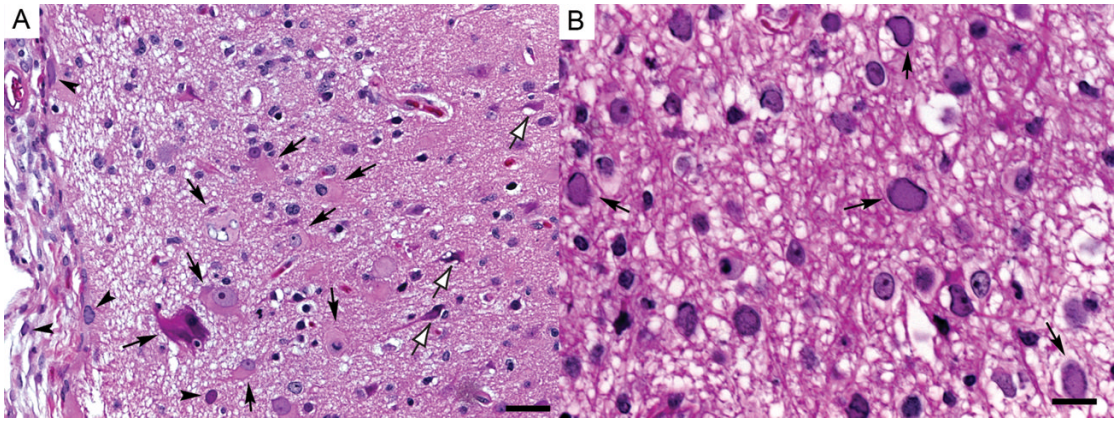

Figure 4.

Histological features of the cerebral lesions. (**A**) Superior temporal gyrus, monkey 22710. Fibroblasts and sparse lymphocytes expand the subarachnoid space. There is a linear subpial zone of edematous neuropil. The molecular and external granular cell layers are hypercellular with numerous gemistocytic and bizarre astrocytes (black arrows), microglial cells and scattered lymphocytes. Scattered fusiform cells in the subarachnoid space and glial cells in the superficial cortex have smudgy amphophilic intranuclear inclusions (black arrowheads). Cortical neurons are shrunken and hyperchromatic (white arrows). Hematoxylin and eosin stain; scale bar = 40 μm. (**B**) Infundibulum, Monkey 22756. Oligodendrocytes have large nuclei containing smudgy amphophilic intranuclear inclusions (black arrows). Hematoxylin and eosin stain; scale bar = 20 μm.

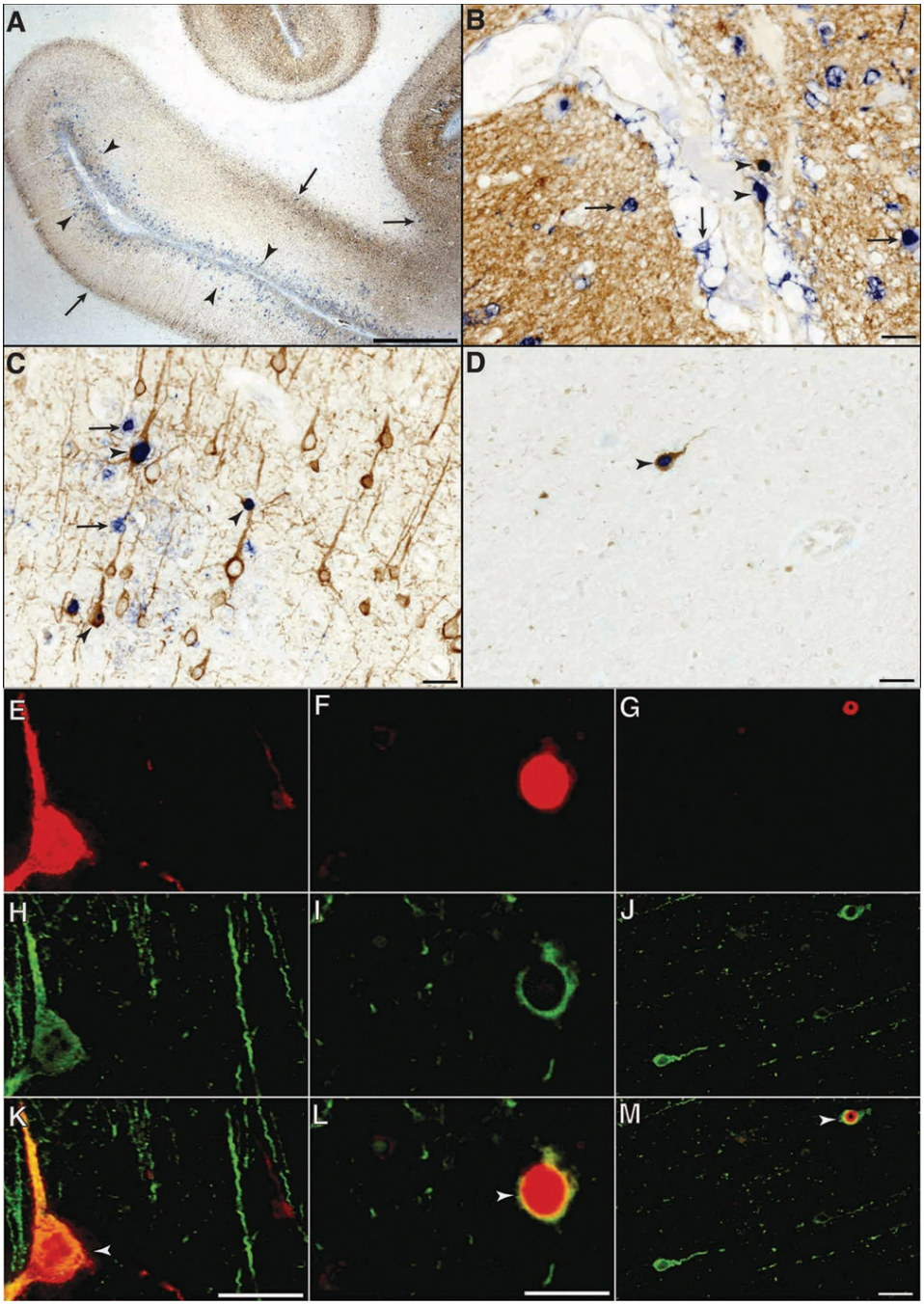

Figure 5.

Characterization of SV40-infected neurons in the cerebral cortex of monkeys by IHC (**A–D**, monkey 22710) and immunofluorescence (**E–M**, monkey 22756). Double IHC staining of neurons (MAP-2, brown) and VP1 protein of SV40-infected cells (PAB597, blue). 3,3′-diaminobenzidine tetrahydrochloride (DAB) and 5-bromo-4-chloro-indolylphosphate/nitroblue tetrazolium (NBT/BCIP; Roche, Indianapolis, IN) were used as chromogens in conjunction with the HRP and alkaline phosphatase (AP) labeled polymers (Envision double stain kit, Dako). Low-magnification view (**A**) shows continuous areas of SV40-infected cells in the external cortex (arrowheads) and at the gray-white junction (arrows, scale bar = 2 mm). Higher magnification shows SV40-infected cells in the meninges and subpial area (**B**, arrows,

scale bar = 5 mm) and SV40-infected cortical neurons (**B, C**, arrowheads). These cells display nuclear or nucleolar SV40 staining and are interspersed with infected glial cells (**C**, arrows, scale bar = 5 mm). Occasionally, isolated SV40-infected neurons were found in the subcortical white matter (**D**, arrowhead, bar = 5 mm). (**E–M**) Double immunofluorescence staining of SV40-infected cells (anti-VFP1 PAB597, Alexa Fluor 568, red, **E–G**) and neurons (MAP-2, Alexa Fluor 488, green, **H–J**) and confirms the presence of multiple SV40-infected cortical neurons (arrowheads, combined images in K–M, scale bar = 5 mm)

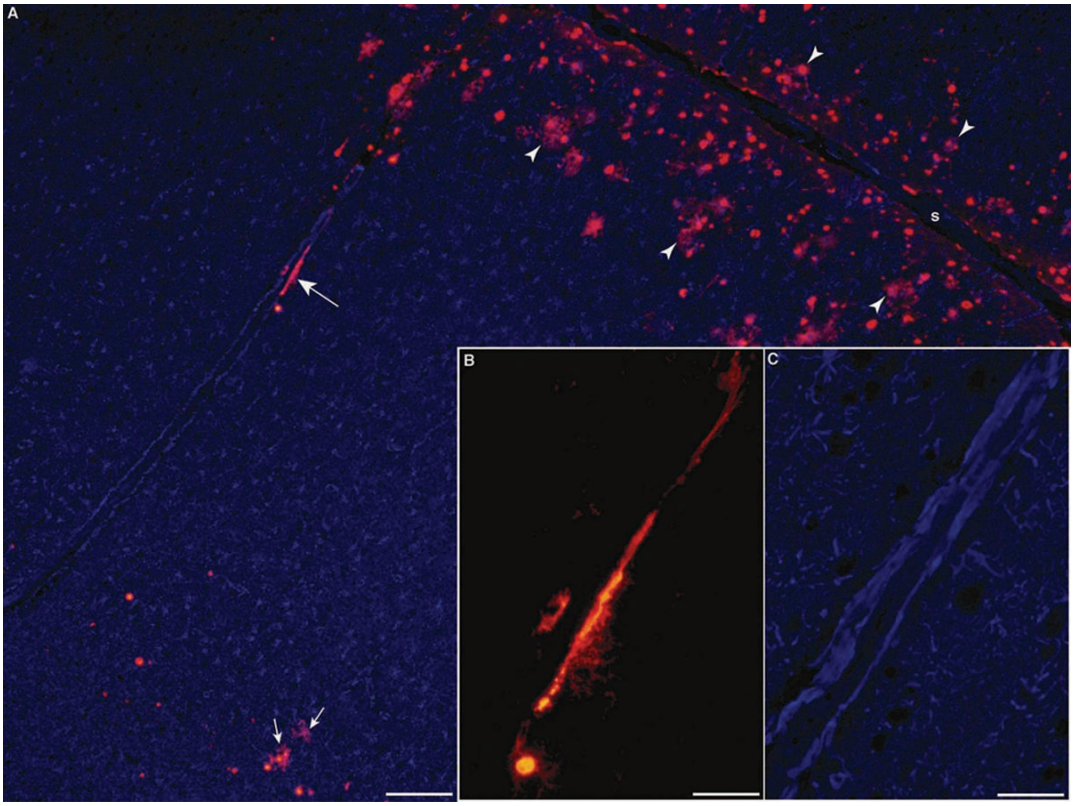

Figure 6.

Characterization of SV40-infected astrocytes in cortical lesions of monkey 22710 by immunofluorescence. (**A–C**) Double immunofluorescence against GFAP (Z0334, Dako) for astrocytes (Alexa Fluor 350, blue) and against VP1 of SV40-infected cells (Alexa Fluor 568, red). (**A**) Numerous SV40-infected astrocytes (purple combination of yellow-red and blue colors) are present mostly in the superficial layers of the cortex (arrowheads) on both sides of a sulcus (S) and in lesser numbers at the gray white junction (short arrows). Some SV40-infected astrocytes were found in mid cortex (long arrow). High magnification insets show the partial colocalization of the astrocytic (**B**, blue, GFAP) and VP1 markers (**C**, red, PAB597, scale bars = 25 mm) in these SV40-infected cells.

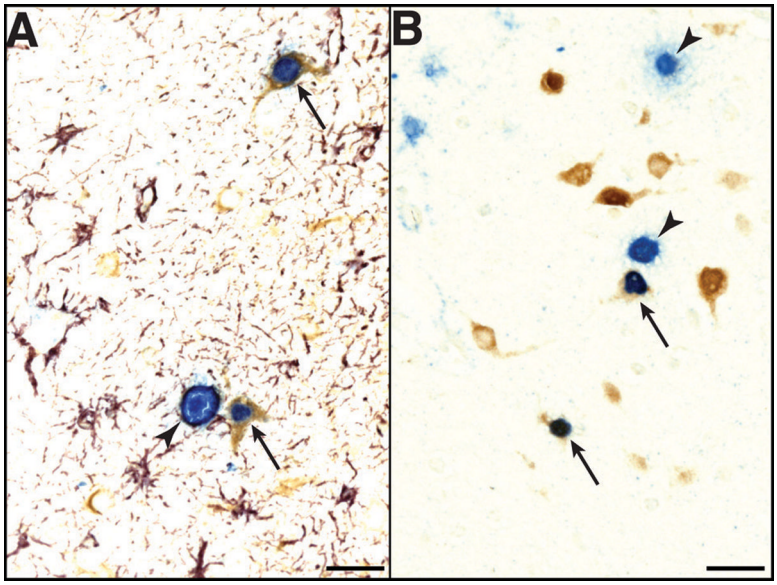

Figure 7.

Colocalization of SV40-infected neurons and astrocytes in the cerebral cortex of monkey. (**A**) Triple IHC staining for neurons (MAP-2, brown), astrocytes (GFAP, purple), and SV40 VP1 protein (Lee Biomolecular Research, blue), shows that SV40-infected neurons (arrows) may be in close proximity to SV40-infected astrocytes (arrowhead). Scale bar 25 mm. (**B**) Double IHC staining for neurons (NeuN, brown) and SV40 VP1 protein (Lee Biomolecular research, blue), reveals SV40-infected neurons (arrows) in the vicinity of SV40-infected glial cells (blue only, arrowheads) interspersed among non-infected neurons. Scale bar = 25 mm.

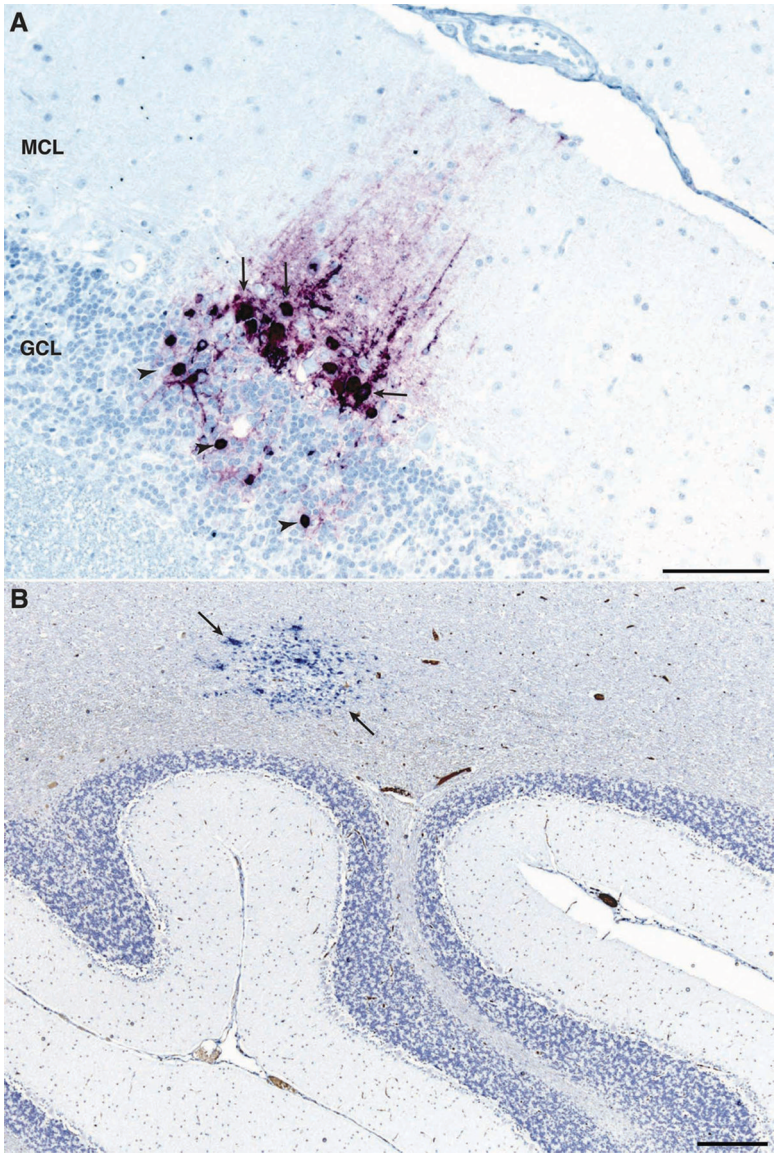

Figure 8.

IHC staining demonstrates focal SV40 infection of the cerebellum in monkey 22710. (**A**) A cluster of cells stain with the anti-VP1 Ab (PAB597, purple) in the cerebellar molecular cell layer (MCL) (arrows) and in the underlying granule cell layer (GCL, arrowheads). Envision G/2 System/AP kit (Dako), Permanent Red chromogen, hematoxylin counterstain, scale bar = 100 mm. (**B**) A focus of SV40-infected glial cells and demyelination is seen in the cerebellar white matter (dark blue, arrows). Envision System/AP kit (Dako), NBT/BCIP chromogen (Roche), hematoxylin counterstain, scale bar = 1 mm.

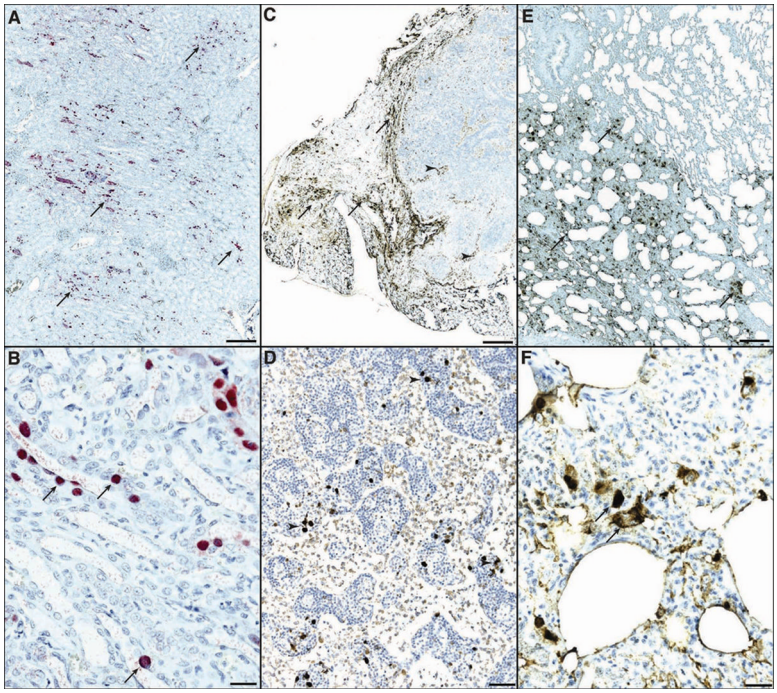

Figure 9.

SV40 infected cells in non-CNS tissues of monkey 22756. (**A, B**) Kidney. Low-power shows tubulointerstitial nephritis with numerous tubulo-epithelial cells stained with the anti-VP1 Ab (purple) (**A**, arrows, scale bar= 1 mm). High-power view of collecting ducts shows SV40-infected tubular cells (purple) with enlarged nuclei (**B**, arrows, scale bar = 2.5 mm). Envision G/2 System/AP kit (Dako), Permanent Red chromogen, and hematoxylin counterstain. (**C, D**) Mesenteric lymph node. Numerous positively stained fusiform mesenchymal cells and histiocytes are present in extracapsular loose areolar connective tissue of the mesentery (brown, arrows) and the sinusoids (brown, arrowheads) (**C**, scale bar= 1 mm). Higher magnification shows scattered SV40-infected cells within medullary cords and sinus histiocytes (**D**, arrowheads, scale bar= 2.5 mm). Advance-HRP kit (Dako), DAB chromogen, hematoxylin counterstain. (**E, F**) Lung. Focal consolidation and interstitial pneumonitis with numerous cells stained with the SV40 Ab (brown, arrows) (**E**, scale bar = 1 mm). Under high power, the SV40-infected cells are morphologically consistent with pneumocytes and alveolar macrophages (brown, arrows) (**F**, scale bar = 2.5 mm). Advance-HRP kit (Dako), DAB chromogen, hematoxylin counterstain.

Table

Single Nucleotide Mutations of $SV40_{CNS1}$ Coding Region Compared to SV40 Prototype 776*

Silent Mutations				aa mutations		
Position	**SV40 prototype 776**	**$SV40_{CNS1}$**	**Position**	**SV40 prototype 776**	**$SV40_{CNS1}$**	**aa change**
732	T	A	1756	A	C	E to D
768	G	C	2792	A	G	S to P
1098	G	A	2895	T	A	E to D
1939	T	A	2918	C	T	D to N
1951	T	C	2950	A	G	I to T
2044	A	C	4839	C	T	A to T
2239	T	G	4879	C	T	M to I
2757	G	A				
2817	G	A				
3930	C	T				

*Abbreviations: aa = amino acids, A = alanine, D = aspartic acid, E = glutamic acid, I = isoleucine, M = methionine, N = asparagine, P = proline, S = serine, T = threonine.